Digital Communications and Networks 9 (2023) 667–676

Contents lists available at ScienceDirect

Digital Communications and Networks

journal homepage: www.keaipublishing.com/dcan

Monte-Carlo based random passive energy beamforming for reconfigurable intelligent surface assisted wireless power transfer☆

Ziyang Lu [a], Yubin Zhao [a,*], Xiaofan Li [b]

[a] School of Microelectronics Science and Technology, Sun Yat-Sen University, Zhuhai, 519082, China
[b] School of Intelligent System Science and Engineering, Jinan University, Zhuhai, 519070, China

ARTICLE INFO

Keywords:
Reconfigurable intelligence surface
Wireless power transfer
Monte-carlo algorithm
Passive beamforming
Gibbs sampling

ABSTRACT

Reconfigurable intelligent surface (RIS) employs passive beamforming to control the wireless propagation channel, which benefits the wireless communication capacity and the received energy efficiency of wireless power transfer (WPT) systems. Such beamforming schemes are classified as discrete and non-convex integer programming problems. In this paper, we propose a Monte-Carlo (MC) based random energy passive beamforming of RIS to achieve the maximum received power of electromagnetic (EM) WPT systems. Generally, the Gibbs sampling and re-sampling methods are employed to generate phase shift vector samples. And the sample with the maximum received power is considered the optimal solution. In order to adapt to the application scenarios, we develop two types of passive beamforming algorithms based on such MC sampling methods. The first passive beamforming uses an approximation of the integer programming as the initial sample, which is calculated based on the channel information. And the second one is a purely randomized algorithm with the only total received power feedback. The proposed methods present several advantages for RIS control, e.g., fast convergence, easy implementation, robustness to the channel noise, and limited feedback requirement, and they are applicable even if the channel information is unknown. According to the simulation results, our proposed methods outperform other approximation and genetic algorithms. With our methods, the WPT system even significantly improves the power efficiency in the nonline-of-sight (NLOS) environment.

1. Introduction

Over the past decades, electromagnetic (EM) waves enable wireless power transfer (WPT) and energy harvesting (EH) turning the wireless signals into an attractive resource for low-power devices [1]. Compared with the near field inductive coupling and resonant coupling WPT technologies which can only transfer power over a short distance, EM based WPT provides more energy broadcasting freedom with a wider and longer range. It is also compatible with wireless communication or the internet of things (IoT) system to prolong the lifetime of mobile devices. With the practical realizations, EM based WPT is becoming popular for commercialized produces, e.g., PowerCast, and even towards to high power applications, e.g., remote powering of unmanned aerial vehicles (UAVs), and space power transfer [2].

To overcome the low efficiency drawback of EM based WPT, MIMO based energy access point is implemented and related energy beamforming methods are applied [3]. The energy beamforming is a typical optimization strategy to control the waveforms on each Tx antenna of the energy access point (E-AP) in order to achieve the maximum available received power or power transfer efficiency (PTE). With more massive antennas employing energy beamforming, the EM power is concentrated in a small area to overcome the path loss [4]. However, deploying massive MIMO requires a huge amount of power amplifiers, antennas, and MCUs for computing, which leads to high cost. Recently, reconfigurable meta-surfaces equipped with low-cost reflecting elements and a control unit, e.g., FPGA, are integrated as reconfigurable intelligence surface (RIS), which effectively adjusts the phase, polarization, frequency, and even the amplitude of the microwave in the air [5]. In this case, the radio propagation channel can be controlled which will bring several potential benefits for the wireless communication systems and IoT systems. Since only passive elements are required which is equivalent to the massive MIMO, the cost is effectively reduced. With RIS, the Tx

☆ This work was partially supported by National Nature Science Foundation of China (No. 62171484), Zhuhai Fundamental and Application Research (No. ZH22017003210006PWC), Fundamental Research Funds for the Central Universities (No. 21621420).

* Corresponding author.
E-mail address: zhaoyb23@mail.sysu.edu.cn (Y. Zhao).

https://doi.org/10.1016/j.dcan.2022.10.031
Received 16 April 2022; Received in revised form 5 August 2022; Accepted 26 October 2022
Available online 12 November 2022

antenna and modulation components are separated and RIS provides a novel modulation method by adapting the phase and polarizing the signal, which is usually named as spatial modulation [6]. In addition, theoretical and experimental investigations indicate that controlling the elements of the RIS also brings performance improvement to the wireless system, which is called passive beamforming [7]. Many researchers study this topic from theoretical [8] and experimental aspects [9] respectively. Thus, with these benefits and the ability to control the EM waveforms, RIS can generate high efficient beam for WPT. In addition, such a beam can even bypass the obstacles and reduce the nonline-of-sight (NLOS) problem [10].

Since the EM waves rely on the passive beamforming or phase shift of RIS to achieve high PTE, the major challenge of RIS is the passive beamforming performance, which includes the PTE and computational complexity [11]. For PTE improvement, it is not difficult to attain the optimal solution when the channel information is available. When such information is unavailable, channel estimation considering RIS phase also helps to develop the optimal solutions. However, such optimal solutions are suitable for continuous phase adaptation of RIS and implemented only in theory [12]. For real RIS implementation, only a fixed set of phrases are controlled for each element. Thus, the passive beamforming is the integer programming problem instead of a continuous convex problem [13]. Some may employ an exhausting method to obtain the optimal results which require a huge amount of computing units and time. Using approximations as the sub-optimal solution is also an option. However, the complexity of approximations is quite similar to the convex optimization but with degraded PTE [14]. Randomized methods generate the solution samples and search for the best result as the final near optimal solution [15]. And these methods even do not require channel information. However, the main challenge of randomized methods is how to generate high quality samples to achieve the optimal results [16]. Take genetic algorithm (GA) for instance, the samples are generated purely randomly and the convergence can not be guaranteed. Instead, importance sampling or related method is preferred. In this paper, we propose a Monte-Carlo based RIS passive beamforming method to achieve the maximum received EM wireless power, which employs Gibbs sampling and re-sampling method for high dimensional beamforming vector samples. The contributions of this paper are summarized as follows:

- We first analyze how the phase shift of the RIS reflective element affects the received energy of the WPT system, which turns into a nonconvex integer programming problem. We obtain the approximation of the RIS reflective elements phase shift vector.
- We propose a Monte-Carlo based RIS passive beamforming method. The Monte-Carlo based random algorithm is executed iteratively to attain the optimal solutions by selecting the local optimal solutions. Such algorithm can be implemented in several scenarios, e.g., with and without channel information. If the channel information is available, even with some estimation errors, we employ an approximation method to provide the passive beamforming with an initial value. Then, Gibbs sampling and re-sampling generate random samplings, and the algorithm chooses the local optimal solution among the random samples as the global optimal solution. We name this algorithm as approximation based random algorithm (AP-RA). If the channel information is unknown and only the total received power is attained, the passive beamforming just controls the RIS with random phase shifts based on the sampling method and compare the beamforming performance to decide the global optimal solution. In this case, we design an online training protocol to implement the algorithm and attain the feedbacks. We name this algorithm as Monte-Carlo randomized algorithm (MC-RA). Our proposed methods are computationally light with fast convergence, and they can be implemented easily in any existed RIS system without further requirements.
- Through theoretical analysis and simulation evaluations, MC-RA and AP-RA have high accuracy, small complexity, and fast convergence rate. The received power attained by AP-RA is 15% larger than GA, and 22% larger than none RIS case. If the channel information is available, AP-RA has a faster convergent rate than MC-RA. If the channel information contains much error, MC-RA outperforms AP-RA since MC-RA does not depend on channel information but on actual received power feedback instead. In the NLOS case, the received power of AP-RA is 246% larger than none RIS case and 91% larger than GA. Thus, in both LOS and NLOS cases, the AP-RA and MC-RA are feasible solutions for passive beamforming of RIS assisted wireless power transfer system.

2. Related work

Passive beamforming is to control the phase shift of each element in RIS to achieve some optimal objects. It is widely used in the WPT and SWIPT. Since such phase shifts are finite discrete values, the passive beamforming is a typical integer programming that is not convex. In this case, several solutions are proposed to divide such a problem into several convex sub-problems. Then iterative algorithms or semi-definite relax (SDR) methods are used as the approximations. Alternative methods may employ machine learning and deep learning methods to approach the optimal solutions for RIS [17].

For WPT, the major goal is to achieve the maximum received power. Mohjazi et al. analyze the WPT battery charging performance using RIS, and provide a statistical charging time model [18]. Tran et al. propose a beam scanning method which employs a multiple antenna transmitter and RIS [19]. Such scanning method consists of two phases, which firstly adapt the beam direction of the transmitter and secondly adapt the phase shifts of RIS to achieve the optimal WPT efficiency. Li et al. investigate the power supply demand of the RIS itself and design a WPT architecture to power up RIS [20]. Tran et al. employ the phase pattern of RIS element array to control the weights of the receiver power levels [21]. Yang et al. study the RIS aided MIMO WPT system model, in which the Tx is equipped with a constant-envelop analog beamformer [22]. And they employ the SDR and the successive convex approximation (SCA) methods as suboptimal solutions.

The passive beamforming is also used to optimize the data rate for SWIPT or WPCN. Considering the fairness among the nodes, the data rate optimization can be turned into the min-max problem. Gong et al. studied the min-max SINR problem in SWIPT with RIS, and propose the branch-and-bound algorithm to solve the related discrete optimization problems [23]. And they also develop two stage scheme to separately optimize the beamforming and phase shifts. Lin et al. propose a joint active and passive beamforming scheme for RIS assist SWIPT system, in which the passive beamforming controls only the on-off state of each RIS reflect element [24]. A double deep Q-network learning based RIS scheduling method is proposed to incorporate with edge computing and wireless power transfer schemes [25]. Yang et al. decompose the max-min rate problem into several sub-problems and propose the sorting and iterative optimization algorithms under the KKT conditions [26]. To deal with the probabilistic constraints of the RIS assist WPCN, the Bernstein-type inequality is introduced and the non-convex problem of passive beamforming is converted into the convex optimization one by using the Dinkelbach's method and matching method [27]. Lin et al. use the passive beamforming scheme to control the on-off state of the RIS for data modulation [28–30]. The ML detection for Rice fading channel is developed as well. Pan et al. propose a block coordinate descent algorithm to achieve the maximum sum data rate of THz SWIPT system [31].

For high power supply, RIS can be used to relay the energy to mobile devices, e.g., UAV. Ren et al. consider the UAV as the remote power transmitter assisted by RIS and propose a beamforming algorithm with trajectory optimization which achieves the minimum energy requirement according to specific locations [32]. Cheng et al. design the minimum scale of RIS and the antenna pattern of UAV to simultaneously charge two UAVs [33].

Note that, the above passive beamforming solutions mainly apply approximations to approach the optimal results. Such methods still require high computational complexity and the actual optimal solution is not achieved. However, randomized solutions are efficient tools for integer programming with proper design. These methods are gradually converged to the optimal results with more and more random samples. Thus, we will introduce how to design the randomized algorithms for passive beamforming in the following contents.

3. System model

The EM based WPT consists of energy-access points (E-APs) and several passive battery-less nodes as illustrated in Fig. 1. We assume that the E-AP with a single antenna is an energy transmitter that transfers energy to all nodes. All the nodes are without batteries, so they are powered by E-AP. The set of nodes is represented by $\mathcal{N}_n = \{1, 2, \ldots, N_N\}$, where N_N represents the number of nodes. The conventional EM based WPT channel is the direct link from the E-AP to the node, and the EM wave that does not reach nodes is wasted. Therefore, we introduce the RIS to reflect EM waves and reduce EM energy waste. The set of RIS reflective elements is represented by $\mathcal{N}_m = \{1, 2, \ldots, N_M\}$, where N_M represents the number of RIS reflective elements. With RIS, the received power of nodes is formulated as

$$\begin{aligned} Y = \sum_{k=1}^{N_N} Y_k + \varrho^H \varrho &= \sum_{k=1}^{N_N} x^H h_k^H h_k x + \varrho^H \varrho \\ &= x^H \boldsymbol{h}^H \boldsymbol{h} x + \varrho^H \varrho \\ &= x^H (\boldsymbol{c} + \boldsymbol{r})^H (\boldsymbol{c} + \boldsymbol{r}) x + \varrho^H \varrho \\ & k \in \mathcal{N}_n \end{aligned} \tag{1}$$

where we use $(\cdot)^H$ to denote the conjugate transpose, Y is the total received power for all EM based WPT nodes; Y_k is the received power of kth node; ϱ is the background noise of EM base WPT system, the magnitude of the background noise is small and does not affect the system analysis and our simulation, so we omit the background noise in the subsequent expression; x is a scalar value instead of a vector that indicates the EM wave transferred from E-AP, which is the E-AP transmit signal; we set $X = x^H x$ as the Tx power of E-AP, assuming that the transmit power X of E-AP to be a constant 30 dBm, i.e., 1 W, it will be more convenient for our subsequent analysis and optimization; $\boldsymbol{h} = [h_1, h_2, \ldots, h_k, \ldots, h_{N_N}]^T$ is the total channel from the E-AP to all nodes, which means that $\boldsymbol{h}$ is a complex vector of dimension $N_N \times 1$; and h_k is the channel from the E-AP to the kth node. For remote WPT, charging is a long process. The received energy of nodes increases with time. In the steady state case, after time t_0, the received energy of all nodes is $Yt_0 = t_0 \sum_{k=1}^{N_N} y_k{}^H y_k = t_0 \sum_{k=1}^{N_N} x^H h_k^H h_k x$. The RIS can reflect EM waves to the node through phase modulation and improve the received power. Here, the channel from E-AP to nodes $\boldsymbol{h}$ is classified as two sub-channels: the channel from the E-AP directly to nodes $\boldsymbol{c}$ and the channel from the E-AP to nodes via the path of RIS $\boldsymbol{r}$. We take the flat fading propagation channel as the channel model [34]. Then, we set $\boldsymbol{c} = [C_1, C_2, \ldots, C_{N_N}]^T$, and C_k is expressed as

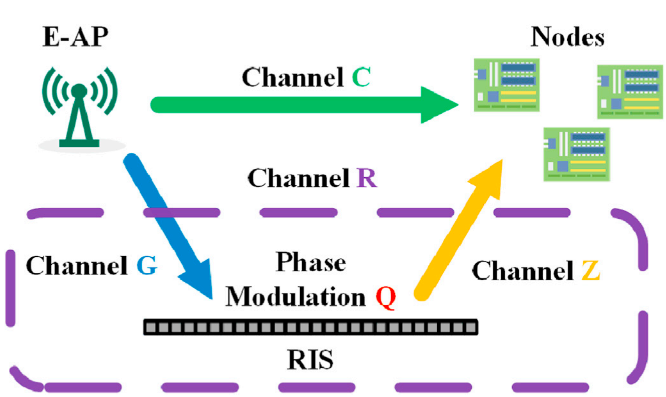

Fig. 1. EM based WPT with RIS.

$$C_k(d_k) = \left(\frac{f_c}{4\pi d_k}\right)^\beta \sqrt{\xi_k} e^{-\frac{j2\pi f_c d_k}{c}} \quad k \in \mathcal{N}_n \tag{2}$$

where d_k is the distance between E-AP and kth node; f_c is the central frequency of the signal; c is the speed of light; β is the fading factor and $\xi_k \in [0, 1]$ is the channel gain of kth path. The channel can be divided into three parts: fading gain, channel gain, and frequency offset. We assume that multipath signals do not cause interference between symbols. Therefore, flat fading propagation can use in both LOS and NLOS cases. We set $\beta_{LOS} = 1$ for LOS case, and $\beta_{NLOS} = 1.2$ for NLOS case. The dimension of the complex vector $\boldsymbol{c}$ is $N_N \times 1$. The mode of the vector $\boldsymbol{c}$ is negatively correlated with distance d_k, and the phase of $\boldsymbol{c}$ is the phase change related to the signal propagation delay.

As illustrated in Fig. 1, the complex vector $\boldsymbol{r} = [R_1, R_2, \ldots, R_{N_N}]^T$ is the channel from the E-AP to nodes. We decompose the channel $\boldsymbol{r} = \boldsymbol{ZQg}$, where $\boldsymbol{g}$ is the channel from the E-AP to RIS; $\boldsymbol{Z}$ is the channel from RIS to nodes; $\boldsymbol{Q}$ is the phase control matrix of RIS. Here, the complex vector $\boldsymbol{g} = [G_1, G_2, \ldots, G_p, \ldots, G_{N_M}]^T$, and each element G_p is formulated as

$$G_p(d_p) = \left(\frac{f_c}{4\pi d_p}\right)^\beta \sqrt{\xi_p} e^{-\frac{j2\pi f_c d_p}{c}} \quad p \in \mathcal{N}_m \tag{3}$$

where d_p is the distance between E-AP and pth reflective element. The channel $\boldsymbol{Z}$ from RIS to the node is $N_N \times N_M$ matrix. The element of the kth row and pth column of the matrix $\boldsymbol{Z}$ is $Z_{k,p}$, which is:

$$\begin{aligned} Z_{k,p}(d_{k,p}) = \left(f_c / [4\pi d_{k,p}]\right)^\beta \sqrt{\xi_{k,p}} e^{-\frac{j2\pi f_c d_{k,p}}{c}} \\ k \in \mathcal{N}_n \quad p \in \mathcal{N}_m \end{aligned} \tag{4}$$

where $d_{k,p}$ is the distance between kth node and pth reflective element. Vector $\boldsymbol{g}$ and matrix $\boldsymbol{Z}$ share the same flat fading propagation channel parameters. The mode of channel vector $\boldsymbol{g}$ and matrix $\boldsymbol{Z}$ are the change in magnitude inversely proportional to the distance, and the phase of elements indicates the propagation delays accordingly.

The diagonal complex matrix $\boldsymbol{Q} = \mathrm{diag}([Q_1, Q_2, \ldots, Q_{N_M}])$ is the phase control matrix of the RIS, and the pth reflective element is

$$Q_p = \rho_p e^{j\psi_p} \quad p \in \mathcal{N}_m \tag{5}$$

where ρ_p is the reflectivity of the reflective element and $\psi_p \in [0, 2\pi)$ is discrete phase shifts of pth reflective element. We set that all reflective elements on RIS are passive $\rho_p \in [0, 1]$. Thus, we can adjust ψ in passive energy beamforming.

4. Problem formulation

The main goal is to achieve the maximum received power Y by adjusting the discrete phase shift vector $\boldsymbol{\psi} = [\psi_1, \psi_2, \ldots, \psi_p, \ldots, \psi_{N_M}]^T$. The problem of maximizing the received power Y is formulated as

$$\begin{aligned}(\mathbb{P}_1):\ &\boldsymbol{\psi}^* = argmaxY\\ &= argmaxx^H\boldsymbol{h}^H\boldsymbol{h}x\\ &\text{s.t.}\ \ X = x^H x \le 1\\ &\psi_p \in \mathcal{N}_{phase}\\ &\rho_p = 1\end{aligned} \tag{6}$$

where $\boldsymbol{\psi}^*$ is the optimal phase shift vector; ψ_p is the pth element of the discrete phase shift vector $\boldsymbol{\psi}$; Y is the total received power for all EM based WPT nodes; $\boldsymbol{h}$ is the channel from the E-AP to nodes; $\boldsymbol{x}$ is a scalar value that represents the EM wave transferred from E-AP and the Tx power $X = \boldsymbol{x}^H x$ should be less than 1; $\mathcal{N}_{phase} = \{\Delta\theta, 2\Delta\theta, \ldots, (F-1)\Delta\theta\}$ is the set of discrete phase shifts. We assume that every reflective element have F states with the same amplitude and an uniform phase shift interval of $\Delta\theta = \frac{2\pi}{F}$. All elements ψ_p take their values from the set $\mathcal{N}_{phase}$. We set all RISs are ideal passive reflect, so the reflectivity of all reflective elements $\rho_p = 1$. Consider the Tx power is constant $X = x^H x = 1$, then $\mathbb{P}_1$ is equivalent to

$$\begin{aligned}(\mathbb{P}_2):\ \ \boldsymbol{\psi}^* &= argmax\boldsymbol{h}^H\boldsymbol{h}\\ &= \sum_{k=1}^{N_N} h_k{}^2\\ s.t.\ &\psi_p \in \mathcal{N}_{phase}\\ &\rho_p = 1\end{aligned} \tag{7}$$

where $||\cdot$ is the modulo operation; $\boldsymbol{h} = [h_1, h_2, \ldots, h_k, \ldots, h_{N_N}]^T$ is the channel from the E-AP to nodes; h_k is the channel from the E-AP to the kth node. Channel from E-AP to nodes $\boldsymbol{h}$ is classified as two sub-channels: the channel from the E-AP directly to nodes $\boldsymbol{c} = [C_1, C_2, \ldots, C_k, \ldots, C_{N_N}]^T$ and the channel from the E-AP to nodes via the path of RIS $\boldsymbol{r} = [R_1, R_2, \ldots, R_k, \ldots, R_{N_N}]^T$. By decomposing the channel element $h_k = C_k + R_k$, $\mathbb{P}_2$ is equivalent to

$$\begin{aligned}(\mathbb{P}_3):\ \ \ \boldsymbol{\psi}^* &= argmax\sum_{k=1}^{N_N} C_k + R_k{}^2\\ &= argmax\sum_{k=1}^{N_N} C_k + \sum_{p=1}^{N_M} Q_p Z_{k,p} G_p{}^2\\ &= argmax\sum_{k=1}^{N_N} C_k + \sum_{p=1}^{N_M} \rho_p e^{j\psi_p} Z_{k,p} G_p{}^2\\ \text{s.t.}\ \ &\psi_p \in \mathcal{N}_{phase}\\ &\rho_p = 1\end{aligned} \tag{8}$$

where $Z_{k,p}$ is the element of the channel matrix $\boldsymbol{Z}$ from RIS to nodes; G_p is the element of the channel vector $\boldsymbol{g}$ from E-AP to RIS; $Q_p = \rho_p e^{j\psi_p}$ is the element of the phase modulation matrix $\boldsymbol{Q}$. The matrix element R_k can be decomposed into $Z_{k,p}$, G_p, and Q_p.

It is observed from $\mathbb{P}_3$ that passive beamforming is an integer programming. A reasonable discrete phase shift vector $\boldsymbol{\psi}$ will maximize the received power Y. Since problem $\mathbb{P}_3$ is a non-convex problem, we apply MC based random algorithm to search for the optimal $\boldsymbol{\psi}^*$.

5. Approximation

The initial value affects the convergent rate of the MC based random algorithms. Therefore, we firstly develop a close form approximation of the integer programming to attain an initial discrete phase shift vector $\boldsymbol{\psi}$. By expanding $|C_k + R_k|^2$, $\mathbb{P}_3$ is equivalent to

$$\sum_{k=1}^{N_N}|C_k+R_k|^2=\sum_{k=1}^{N_N}(C_k+R_k)^H(C_k+R_k)=\sum_{k=1}^{N_N}(C_k{}^H C_k+C_k{}^H R_k+C_k R_k{}^H+R_k R_k{}^H) \tag{9}$$

Assuming that the positions of E-AP and nodes are already known, and channel C_k is fixed, $C_k{}^H C_k$ does not have an impact on the received power when only the phase modulation matrix $\boldsymbol{Q}$ is adjusted. Since the magnitude of the channel is negatively correlated with the distance d, the magnitude of the channel vector $\boldsymbol{c}$ is greater than $\boldsymbol{r}$. Therefore, the magnitude of $R_k R_k{}^H$ is less than $C_k R_k{}^H$. Omitting $C_k{}^H C_k$ and $R_k R_k{}^H$, Eq. (9) is approximated as

$$\sum_{k=1}^{N_N}(C_k{}^H R_k + C_k R_k{}^H) = 2\Re\left\{\sum_{k=1}^{N_N}(C_k{}^H R_k)\right\} \tag{10}$$

where $\Re\{\cdot\}$ is the real part of the complex value. Equation (10) indicates that the real part of $C_k{}^H R_k$ is associated with the received power. By rearranging the order of the summation, Eq. (10) is equivalent to

$$\begin{aligned}2\Re\left\{\sum_{k=1}^{N_N}(C_k{}^H R_k)\right\} &= 2\Re\left\{\sum_{k=1}^{N_N}\left(C_k{}^H\sum_{p=1}^{N_M} Q_p Z_{k,p} G_p\right)\right\}\\ &= \sum_{p=1}^{N_M} 2\Re\left\{Q_p G_p \sum_{k=1}^{N_N}(Z_{k,p} C_k{}^H)\right\}\end{aligned} \tag{11}$$

where the element R_k is decomposed into $\sum_{p=1}^{N_M} Q_p Z_{k,p} G_p$. Then, in order to attain maximum $\Re\left\{\sum_{k=1}^{N_N}(C_k{}^H R_k)\right\}$, we just need to maximize $\Re\left\{Q_p G_p \sum_{k=1}^{N_N}(Z_{k,p} C_k{}^H)\right\}$. Removing the summation symbol from Eq. (11), we obtain

$$\begin{aligned}(\mathbb{P}_4):\ \ \boldsymbol{\psi}^* &= argmax\Re\left\{Q_p G_p \sum_{k=1}^{N_N}(Z_{k,p} C_k{}^H)\right\}\\ &= argmax\Re\{\rho_p e^{j\psi_p} L_p\}\\ \text{s.t.}\ \ &p \in \mathcal{N}_m\\ &\psi_p \in \mathcal{N}_{phase}\\ &\rho_p = 1\end{aligned} \tag{12}$$

where $L_p = G_p \sum_{k=1}^{N_N}(Z_{k,p} C_k{}^H)$; ψ_p is the pth element of the discrete phase shift vector $\boldsymbol{\psi}$.

According to $\mathbb{P}_4$, the total received power of all nodes Y is maximized when the real part of $\Re(e^{j\psi_p} L_p)$ reaches its maximum value. Since the phase of $e^{j\psi_p}$ is opposite to L_p, $\Re(e^{j\psi_p} L_p)$ have only a real part and no imaginary part. Therefore, Y is maximized when the phase modulation parameter ψ_p is equal to the phase of $L_p{}^H$. Then, the approximated discrete phase shift element ψ_p^* in discrete phase shift vector $\boldsymbol{\psi}^*$ is expressed as

$$\psi_p^* = \left\lfloor \frac{arctan\left(\frac{\Im\{L_p{}^H\}}{\Re\{L_p{}^H\}}\right)}{\Delta\theta} + \frac{1}{2}\right\rfloor \cdot \Delta\theta \quad p \in \mathcal{N}_m \tag{13}$$

where $\arctan(\cdot)$ is the arctangent operation; $\Im\{\cdot\}$ is the imaginary part of the complex number; $\lfloor\rfloor\cdot$ is floor operation. By using Eq (13), we obtain an initial discrete phase shift vector $\boldsymbol{\psi}^*$ for the MC based random algorithm.

6. Monte-Carlo based random algorithm

Controlling the discrete phase of RIS to achieve the maximum received power belongs to the integer programming problem, in which the randomized algorithm is an effective and fast implement solution. Here, we apply the Monte-Carlo (MC) sampling method to randomly generate random discrete phase shift vector samples due to its sample diversity and fast convergence features. The MC algorithm is an iterative algorithm which employs several random samples to simulate the distribution of a system. The distribution can be a probability density function or a typical calculation result set. If the sample set is sufficiently large, the approximated distribution is approaching the actual distribution. Then, final results are attained according to different objects based on such distribution. According to the RIS passive beamforming features, our algorithm consists of phase modulation vector generation, performance evaluation, and re-sampling. Considering the WPT system may have or without knowledge of wireless propagation channel, we design two MC based random algorithms with and without channel information for RIS assisted WPT.

6.1. With channel information

With perfect channel information, we can obtain the ideal channel model $\boldsymbol{h}$. Here, we employ the ideal channel $\boldsymbol{h}$ as the reference to derive the approximated discrete phase shift vector $\boldsymbol{\psi}^*$ as calculated in Eq. (13), which is the initial sample. Then, the Gibbs sampling and re-sampling methods are applied. The optimal solution is the sample with the maximum received power. We define the MC based random algorithm using approximation with channel knowledge as the approximation based random algorithm (AP-RA).

6.1.1. Initial sampling

We initially generate a phase modulation vector sample set $\{\boldsymbol{\psi}_1^q\}_{q=1}^{M_S}$ for AP-RA. Here, we assume that a phase modulation vector sample set $\{\boldsymbol{\psi}_t^q\}_{q=1}^{M_S}$ is the tth sample set, which consists of M_S vectors. From Eq. (13), we obtain discrete phase shift vector $\boldsymbol{\psi}^*$. We set that all the initial phase modulation vector $\boldsymbol{\psi}_1^q = \boldsymbol{\psi}^*$. Therefore, the generation of initial sample sets $\{\boldsymbol{\psi}_1^q\}_{q=1}^{M_S}$ depends on the channel information.

6.1.2. Gibbs resampling

For each $\boldsymbol{\psi}_t^q$, there is a total received power Y_t^q according to Eq. (1). Then, we form a new set $\{Y_t^q\}_{q=1}^{M_S}$ in each iteration as the indicator for phase vector sample $\{\boldsymbol{\psi}_t^q\}_{q=1}^{M_S}$ selection. All samples $\{\boldsymbol{\psi}_t^q\}_{q=1}^{M_S}$ are sorted in descending order according to the received power level of $\{Y_t^q\}_{q=1}^{M_S}$. Note that, such calculation is executed only on the RIS side due to the channel information is known. Then, only $N_S < M_S$ samples with the highest Y_t^q are selected, and we use the selected samples $\{\tilde{\boldsymbol{\psi}}_t^v\}_{v=1}^{N_S}$ as seed to generate new samples for next step of calculation iteratively.

In order to avoid the sample impoverishment and increase the diversity, we still employ Gibbs resampling to generate new samples. We generate random sample set $\{\boldsymbol{\psi}_{t+1}^q\}_{q=1}^{M_S}$ from selected sample set $\{\tilde{\boldsymbol{\psi}}_t^v\}_{v=1}^{N_S}$. The random sample is drawn as

$$\psi_{t+1}^q[j] = \tilde{\psi}_t^v[j] + \beta_t^q[j]P_t^q[j]\Delta\theta \quad j \in \mathcal{N}_m \tag{14}$$

where $\boldsymbol{\psi}_{t+1}^q$ is the qth vector in sample set $\{\boldsymbol{\psi}_{t+1}^q\}_{q=1}^{M_S}$; $\psi_{t+1}^q[j]$ is the jth element in vector $\boldsymbol{\psi}_{t+1}^q$; $\tilde{\psi}_t^v[j]$ is the jth element in selected sample vector $\tilde{\boldsymbol{\psi}}_t^v$; $\beta_t^q[j] \in \{0,1\}$ is the control factor for $\psi_{t+1}^q[j]$; $P_t^q[j] \in \{-N_l, \ldots, 0, \ldots, N_l\}$ is the random perturbation value; $\Delta\theta$ is an uniform phase shift interval. We only selected N_S elements $\tilde{\psi}_t^v[j]$ to generate random values. The new samples $\boldsymbol{\psi}_{t+1}^q$ are near to the previous samples $\tilde{\boldsymbol{\psi}}_t^v$. Therefore, perturbations should not keep new samples too far away. For each vector $\tilde{\boldsymbol{\psi}}_t^v$ from $\{\tilde{\boldsymbol{\psi}}_t^v\}_{v=1}^{N_S}$, we generate $\frac{M_S}{N_S}$ vectors based on Eq. (14). Then, the sample set $\{\boldsymbol{\psi}_{t+1}^q\}_{q=1}^{M_S}$ is able to be generated from selected sample set $\{\tilde{\boldsymbol{\psi}}_t^v\}_{v=1}^{N_S}$, and it is used for the next iteration.

Algorithm 1 Approximation based Random Algorithm (AP-RA)

```
Initialize sample set {ψ_1^q}_{q=1}^{M_S} by using approximation;
for Number of iterations t = 1 : N_i do
    for Parameter vectors q = 1 : M_S do
        Calculate received power Y_t^q base on (1);
    end for
    // Re-Sample;
    Sort {ψ_t^q}_{q=1}^{M_S} base on received power {Y_t^q}_{q=1}^{M_S}
    Chose N_S parameter vectors {ψ̃_t^v}_{v=1}^{N_S};
    Re-generate vectors {ψ_{t+1}^q}_{q=1}^{M_S} from {ψ̃_t^v}_{v=1}^{N_S} based on (14)
end for
Choose vectors ψ̃_{N_i}^v with maximum Y_{N_i}^q
Output: ψ* = ψ̃_{N_i}^v
```

The whole algorithm is illustrated in Algorithm 1. First based on the sample set $\{\boldsymbol{\psi}_t^q\}_{q=1}^{M_S}$, the received power Y_t^q is calculated. By Gibbs resampling, the vector set $\{\boldsymbol{\psi}_{t+1}^q\}_{q=1}^{M_S}$ can be regenerated for the next iteration. Finally, the sample $\tilde{\boldsymbol{\psi}}_{N_i}^v$ under the maximum received power $Y_{N_i}^q$ is selected as the optimal $\boldsymbol{\psi}^*$.

6.2. With imperfect channel information

Note that the channel information may contain errors due to the imperfect channel estimation. However, MC based random algorithm is still applicable to search for the discrete phase shift vector $\boldsymbol{\psi}$ in this case. Then the channel matrix with imperfect channel information is expressed as

$$\hat{\boldsymbol{h}} = \boldsymbol{h} + \boldsymbol{\xi} \tag{15}$$

where $\boldsymbol{h}$ is the ideal channel vector; $\boldsymbol{\xi} = [\xi_1 \cdots \xi_k \cdots \xi_{N_N}]^T$ is the noise vector with dimension $N_N \times 1$ and ξ_k is the kth element. We can still employ AP-RP to derive the optimal phase shift vector based on $\hat{\boldsymbol{h}}$, in which the initial approximation and the calculation of $\{Y_t^q\}_{q=1}^{M_S}$ are attained based on $\hat{\boldsymbol{h}}$ in Eqs. (13) and (1). However, the channel estimation noise will degrade the final results.

6.3. Without channel information

If the channel information is absent, the initial approximation solution in AP-RA is not available. In addition, $\{Y_t^q\}_{q=1}^{M_S}$ cannot be calculated on the RIS side, but it can be attained via feedbacks from nodes, where each node sends the received power value to the RIS. According to this strategy, we convert the iterations into a time sequential periods. Then, we design an online training protocol as illustrated in Fig. 2. There are N_i periods for calculation, and each period contains M_S slots. Each slot represents a discrete phase shift vector sample $\boldsymbol{\psi}_t^q$. In each slot, RIS performs $\boldsymbol{\psi}_t^q$ and receives the power feedback from the nodes to attain the sum power Y_t^q. By the end of each period, the MC algorithm executes Gibbs re-sampling and executes the new samples for the next period. Our proposed online training protocol is an interactive process of asymptotic optimization. Despite the high complexity drawback, IoT devices which

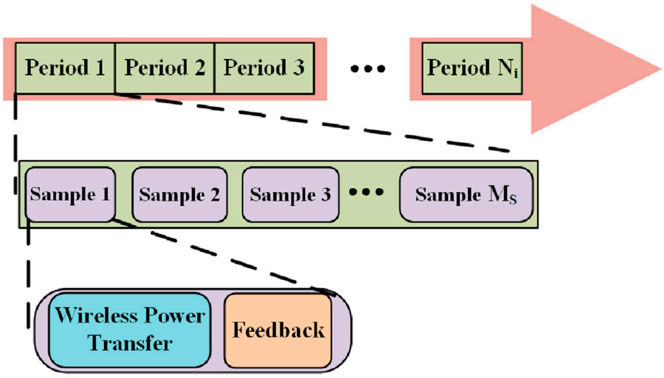

Fig. 2. Online training protocol for passive energy beamforming.

use WPT as energy supplier need a long term of remote charging. And such charging is rather static. In this case, the training phase is still short compared with the long charging time. In addition, the WPT is not as demanding as communication in terms of information transmission rate and accuracy. Therefore, our proposed online training protocol is still applicable to practical IoT WPT scenarios. Since such an algorithm is a pure randomized method without approximation, we name it as Monte-Carlo based random algorithm (MC-RA).

The MC-RA for no channel information is presented in Algorithm 2. We generate an initial random sample set of parameter vectors $\{\psi_1^q\}_{q=1}^{M_S}$, the Gibbs sampling and re-sampling are still used as in Algorithm 1. However, $\{Y_t^q\}_{q=1}^{M_S}$ is the actual power feedback instead of calculating results in AP-RA. In this case, MC-RA is robust to the channel noise but consumes time and communication overhead.

Algorithm 2 Monte-Carlo based Random Algorithm (MC-RA)

1: Random generate initial sample set $\left\{\psi_1^q\right\}_{q=1}^{M_S}$
2: **for** Number of periods $t = 1 : N_i$ **do**
3: **for** Parameter vectors $q = 1 : M_S$ **do**
4: Measure received power $\left\{Y_t^q\right\}_{q=1}^{M_S}$ of nodes based on feedback;
5: **end for**
6: // Re-Sample;
7: Sort $\left\{\psi_t^q\right\}_{q=1}^{M_S}$ base on received power $\left\{Y_t^q\right\}_{q=1}^{M_S}$;
8: Chose N_S parameter vectors $\left\{\widetilde{\psi}_t^v\right\}_{v=1}^{N_S}$;
9: Re-generate vectors $\left\{\psi_{t+1}^q\right\}_{q=1}^{M_S}$ from $\left\{\widetilde{\psi}_t^v\right\}_{v=1}^{N_S}$ based on (14)
10: **end for**
11: Choose vectors $\widetilde{\psi}_{N_i}^v$ with maximum $Y_{N_i}^q$
12: Output: $\psi = \widetilde{\psi}_{N_i}^v$

7. Performance analysis

7.1. Convergence analysis

The convergence rate of the MC based random algorithm is determined by the number of samples and the number of iterations. In the classical Monte-Carlo algorithm, the convergence rate is proportional to the square of the number of samples $M_S{}^2$ [35], in which the variance between the received power distribution and the true stationary distribution is expressed as

$$\|\mathrm{normalize}[\boldsymbol{Y}(\boldsymbol{\psi})] - \pi(\cdot)\|_{\mathrm{var}} \le \varsigma\left(\frac{1}{M_S{}^2}\right)^{N_i} \tag{16}$$

where $\mathrm{normalize}[\cdot]$ is the normalization operation which normalize it by its 1-norm; $\boldsymbol{Y}(\boldsymbol{\psi})$ is the receive power set for sample set $\boldsymbol{\psi}$; $\pi(\cdot)$ is the true smooth distribution; the coefficient $\varsigma > 0$ depends on the sample dimension; M_S is the number of samples; N_i is the number of iterations. From Eq. (16), coefficient ς depends on the sample dimension, which is the number of reflective elements of the RIS. If the number of reflective elements of RIS rises, a larger M_S and N_i are required. When M_S and N_i are infinite, the received energy $\boldsymbol{Y}(\boldsymbol{\psi})$ can reach $\pi(\cdot)$. In the real implementation, we properly chose the values of M_S and N_i when the performance is approaching the optimal result.

7.2. Accuracy

The MC based random algorithm is randomly sampled, according to the Lindburg-Levy theorem in probability theory, the sample sum of each iteration obeys the standard normal distribution $\mathcal{N}(0,1)$ [36]

$$\lim_{N_i\to\infty}\Pr\left(\frac{\tilde{Y}-\mu}{\sigma/\sqrt{N_i}} < X_a\right) = \int_{-\infty}^{X_a}\frac{1}{\sqrt{2\pi}}e^{-t^2/2}dt \tag{17}$$

where $\Pr(\cdot)$ is expressed as the probability, N_i is iteration number of the MC based random algorithm, $\mu = \mathbb{E}_Y(Y)$ is the expected value of the received power Y, σ is the mean squared deviation of the received power Y, $\tilde{Y}$ is the estimation of Y, and X_a is called the standard normal distribution difference. The value of X_a is related to the confidence level. We set the confidence level to 0.95, and by checking the confidence interval z-value conversion table, we can get the standard normal distribution difference $X_a = 1.96$. For our proposed MC based random algorithm, the estimate $\tilde{Y}$ using Gibbs resampling is only correlated with the maximum received power Y. We assume the $\tilde{Y}$ is expressed as

$$\tilde{Y} = \max\left[\boldsymbol{Y}\left(\{\boldsymbol{\psi}_{N_i}^q\}_{q=1}^{M_S}\right)\right] \tag{18}$$

where $\boldsymbol{Y}\left(\left\{\boldsymbol{\psi}_{N_i}^q\right\}_{q=1}^{M_S}\right)$ is the received power set of parameter vectors $\left\{\boldsymbol{\psi}_{N_i}^q\right\}_{q=1}^{M_S}$; $\max[\cdot]$ is the operation of taking the maximum value. The absolute error ϵ_a of the estimate of the received power Y with the confidence interval $\left(\tilde{Y}-\epsilon_a, \tilde{Y}+\epsilon_a\right)$ is

$$\epsilon_a = \frac{X_a\sigma}{\sqrt{N_i}} \tag{19}$$

Therefore, the relative error of the received power Y is expressed as

$$\epsilon_r = \frac{\epsilon_a}{\tilde{Y}} = \frac{X_a\sigma}{\tilde{Y}\sqrt{N_i}} \tag{20}$$

The relative error of the received power Y is related to the number of iterations N_i. When the number of iterations is larger, the relative error is smaller and the estimated value of the received power $\tilde{Y}$ is more accurate.

7.3. Complexity

The complexity of an algorithm leads to the running time of the algorithm. For the MC based random algorithm, the complexity of Gibbs resampling is $\mathcal{O}(M_S\log_2(M_S))$, so the complexity of the algorithm with N_i iterations is $\mathcal{O}(N_iM_S\log_2(M_S))$ [37]. For the exhausting algorithm, the complexity is $\mathcal{O}(F^{N_M})$. Comparing the complexity of the two algorithms, we can get that the complexity of the MC based random algorithm is much smaller than the exhausting algorithm.

We assume that the number of RIS reflective elements $N_M = 2000$ and each reflective element contains $F = 8$ discrete phase shifts. The iteration number of Monte-Carlo random algorithm $N_i = 200$ and the node number of Gibbs resample $M_S = 50$. Therefore, the complexity of exhausting algorithm is $\mathcal{O}(1.51 \times 10^{1806})$, much larger than Monte-Carlo random algorithm $\mathcal{O}(5.64 \times 10^4)$.

7.4. Convergence rate

When we design iterative algorithms, it is inevitable to mention the convergence rate. The analytical expression for the convergence rate is

$$\lim_{k\to\infty}\frac{\left\|(\boldsymbol{\psi})_k - \boldsymbol{\psi}^*\right\|}{\left\|(\boldsymbol{\psi})_{k-1} - \boldsymbol{\psi}^*\right\|} = C \tag{21}$$

where $(\boldsymbol{\psi})_k$ is the phase shift vector of k iterations and $\boldsymbol{\psi}^*$ is the optimal phase shift vector. When the constant $C = 1$, we can call $\boldsymbol{\psi}$ sublinear convergence; when $0 < C < 1$, we can call $\boldsymbol{\psi}$ linear convergence [38]. Since we are analyzing an iterative algorithm, the convergence rate Eq. (21) can be expressed as

$$\lim_{k\to\infty}\frac{\left\|(\boldsymbol{\psi})_k - \boldsymbol{\psi}^*\right\|}{\left\|(\boldsymbol{\psi})_{k-1} - \boldsymbol{\psi}^*\right\|} = \lim_{k\to\infty}\frac{\left\|(\boldsymbol{\psi})_{k-1} + \mathbb{E}_{\varphi}(\boldsymbol{\varphi}_k) - \boldsymbol{\psi}^*\right\|}{\left\|(\boldsymbol{\psi})_{k-1} - \boldsymbol{\psi}^*\right\|} \tag{22}$$

where $\mathbb{E}_{\varphi}(\boldsymbol{\varphi}_k)$ is the expected value of the iterative increase of $(\boldsymbol{\psi})_{k-1}$. Since the iteration of the exhausting algorithm is random, so $\mathbb{E}_{\varphi}(\boldsymbol{\varphi}_k) = 0$ and $C = 1$. The iteration of the MC based random algorithm is based on the descending order, so $\|\mathbb{E}_{\varphi}(\boldsymbol{\varphi}_k)\rangle 1$ and $C < 1$. Therefore, we can analyze that the exhausting algorithm is sublinear convergence; the MC based random algorithm is linear convergence. The convergence rate of MC based random algorithm is greater than that of the exhausting algorithm.

8. Simulations

In this section, we illustrate the received power comparisons via simulations in 3 scenarios: passive beamforming with perfect channel information, passive beamforming with imperfect channel information, and passive beamforming without perfect channel information. As shown in Fig. 3, the playing field of EM base WPT system is restricted to a 100×100 m^2 square region $\mathcal{A}$. The E-AP, nodes, and RIS are in the region $\mathcal{A}$, and E-AP is located at the origin. For better reflection of EM waves, we set the coordinates of two RIS at (50, 0) and (50, −50), respectively. Our proposed Monte-Carlo based passive beamforming algorithm can apply to every RIS placement case, even though all RIS reflective elements are decentralized. We obtain the channel information from the coordinates of reflective elements. Therefore the topological structure of the RIS does not affect the computation of channel information or the use of the algorithm. All nodes are randomly distributed in the region $\mathcal{A}$ in each simulation. The single antenna of E-AP emits EM waves at 2.4 GHz and the Tx power is 30 dBm. The reflectivity of RIS is set as $\rho = 1$ and the uniform phase shift interval is $\pi/4$, then each reflective element has 8 different phase modulations $\{\frac{k\pi}{4}\}_{k=0}^{7}$. The element spacing of RIS is $\frac{\lambda}{5}$, where λ is the wavelength of the EM wave. We use 400 Monte-Carlo simulations in each simulation and average the results of total received power.

8.1. With channel information & without channel information

Here, the simulations are performed for two cases: Firstly, the channel information among E-AP, RIS, and nodes is perfectly known to the system; and secondly, all the channel information is unknown but only the total received power is attained. In the first case, we implement the proposed AP-RA to control RIS. We use approximation to generate the initial sample with channel information. Using this sample set as the input of AP-RA, the optimal phase modulation vector for the case with perfect channel information is attained iteratively. For the second case, we implement MC-RA to control RIS. Since without channel information, we just generate a random sample set of phase modulation parameters as the input of MC-RA. The optimal phase modulation vector without channel information is obtained according to the maximum total received power. We analyze the effects of the number of RIS, the number of iterations, and the number of samples on the received power of the nodes. In this simulation, the wireless propagations among E-AP, RIS, and nodes are LOS and the noise is neglected. We implement our proposed AP-RA and MC-RA, and also compare them with the approximate solution algorithm (AP) and genetic algorithm (GA), which is a classical random optimization algorithm.

First, we formulate the received power optimized by four different passive beamforming algorithms with the received power without RIS in Fig. 4. The number of nodes is 20, and we set the number of samples for each algorithm $M_S = 50$. Then we set the iteration number of all the stochastic optimization algorithms as 200.

As illustrated in Fig. 4, we observed the rise of the received power of the EM based WPT system when the number of RIS is increased from 200 to 2000. With more the number of RIS elements, the received power of all the algorithms are increased accordingly. Due to the high iterations, the received power of applying the AP-RA is slightly larger than MC-RA, but both of them are much larger than AP and GA. This indicates that the MC based random algorithms outperform the GA algorithm in enhancing the received power of the RIS assisted WPT system model.

Next, we compare the difference in received power between three passive beamforming random optimization algorithms with the different number of iterations. We implement and proposed AP-RA and MC-RA, which compare with GA. We deploy 20 nodes randomly in the playing

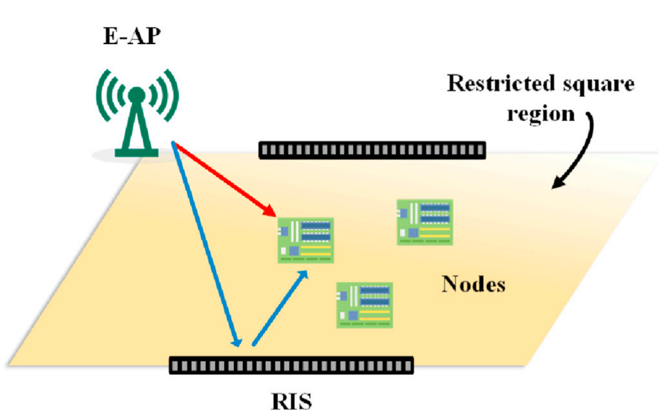

Fig. 3. System simulation for EM based WPT system.

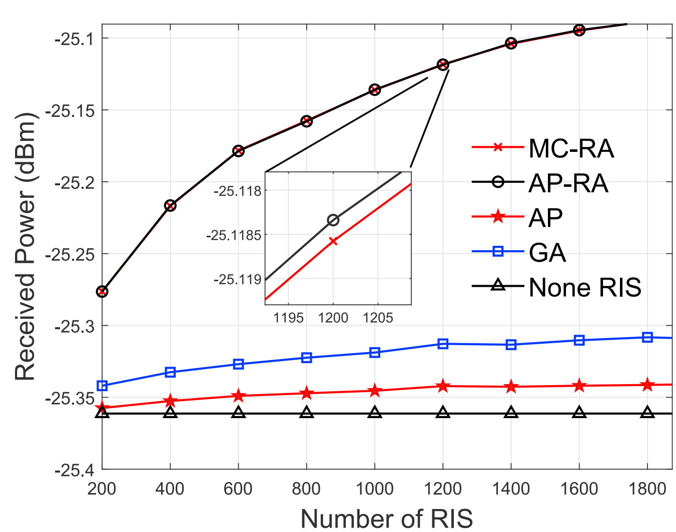

Fig. 4. Received power with different number of RIS reflective elements.

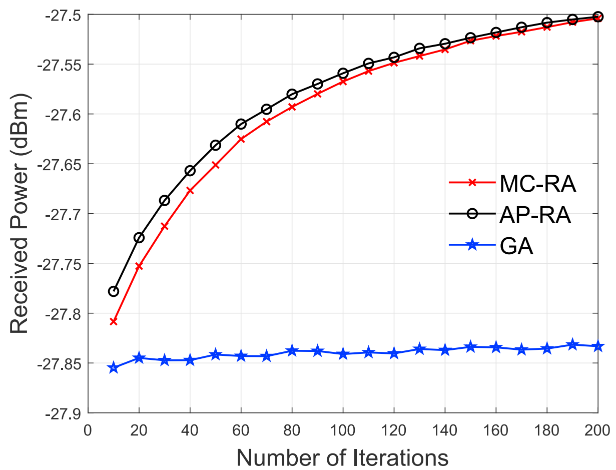

Fig. 5. Received power with different number of iterations.

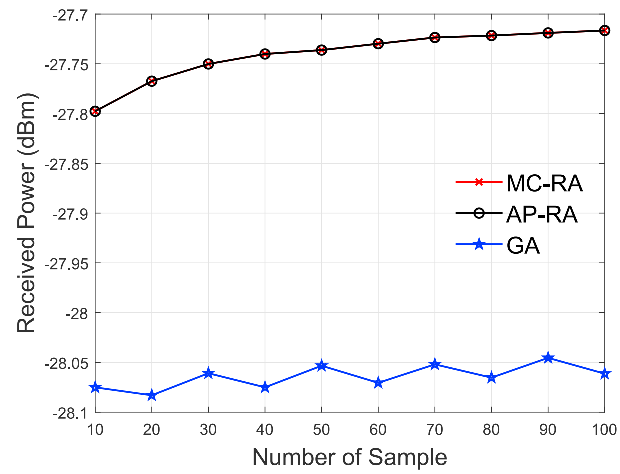

Fig. 6. Received power with different number of sample.

field and set the number of samples of the algorithm $M_S = 50$. Fig. 5 demonstrates a plot of the different iteration numbers versus the total received power. With more number of iterations, the total received power of all the algorithms are approaching their own maximum values. When the number of iterations reaches 200, the received power of AP-RA with approximation as the initial value is almost the same as MC-RA. This indicates that when the number of iterations gradually increases, the improvement of WPT system performance due to channel information gradually decreases, and the Monte-Carlo based random algorithm can optimize the RIS assisted WPT system in the absence of channel information feedback. The received power of AP-RA is greater than MC-RA under the same number of iterations, which indicates that the approximation provides efficient initial samples to make the algorithm fast convergent. The received power of both AP-RA and MC-RA are much larger than GA, which demonstrates the advantages of MC based algorithm in both convergence and performance. For remote WPT system, charging is a long process. The operation of the algorithm is a short time process compared to charging. Therefore, the algorithm's operation time does not significantly affect the performance of the remote WPT system. Meanwhile, the MC-RA is simple to apply and a correspondingly fast algorithm. In our simulation, it takes only 170 ms to execute MC-RA with 200 iterations without the WPT system simulation, i.e., only 0.8 ms per iteration. We can attain in Fig. 5 that the performance improvement of the WPT system starts to decrease as the number of iterations increases. For practical WPT system, the performance improvement of WPT system is quite cost-effective when the number of MC-RA iterations is 100. Such setting only takes 80 ms, which satisfies the demand of a practical WPT system.

Then we simulate the difference in received power between the three passive beamforming random optimization algorithms for the different number of samples. We implement and proposed AP-RA and MC-RA, which compare with GA. We set that there are 20 nodes; the iteration number of the algorithm is 200; the number of RIS phase modulation units is 800. Fig. 6 depicts a plot of the number of samples versus received power. When the number of iterations is up to 200, the received power of the MC-RA algorithm is approximately the same as that of the AP-RA algorithm, and both are much larger than GA algorithm. This indicates that the MC based random algorithm is better than the GA algorithm in increasing the received power of the EM based WPT system model. However, increasing the number of samples does not improve too much, which means that the iterations play a dominant factor in convergence rather than the number of samples.

For remote WPT, the attained power is rather low and the improvement based on beamformings is even smaller. However, such improvement is more valuable if the quantified power level improvement is converted into percentile. It can be observed from Figs. 4–6 that the average received power of AP-RA is 0.3 dBm greater than GA. It claims that the average power increase rate between AP-RA and GA is 15%, which can prove that our proposed MC based passive beamforming algorithm significantly improves the received power of the WPT system.

8.2. Imperfect channel information

Consider the imperfect channel case where the channel estimation contains noise, then $\hat{\boldsymbol{h}} = \boldsymbol{h} + \boldsymbol{\xi}$, where $\boldsymbol{h}$ is the ideal channel vector and $\boldsymbol{\xi}$ is the noise vector. Here, each element of the noise matrix follows zero-mean Gaussian distribution $\xi_k = \frac{h_k}{\sqrt{\mathrm{SNR}}}\mathcal{N}(0, \sigma^2) \quad k \in \mathcal{N}_n$, where σ^2 is the variance; h_k is the kth element of the ideal channel vector $\boldsymbol{h}$ and SNR is the signal-to-noise ratio of the channel information. Then we use SNR to indicate the channel estimation performance. AP-RA employs $\hat{\boldsymbol{h}}$ to derive an initial passive beamforming solution and generates samples accordingly. MC-RA is executed still based on the actual feedback. In this simulation, we evaluate the relationship between the SNR and the received power.

We compare the received power of four different passive beamforming algorithms, and we also evaluate the received power in the case without RIS. We implement and proposed AP-RA and MC-RA, which compare with AP and GA. We deploy 20 nodes, and set the number of samples for the algorithm $M_S = 50$. The iteration number for all the optimization algorithms is 200. In addition, the number of RIS phase modulation cells is 800. In this simulation, no obstacles are presented among all E-AP, RIS, and nodes, thus we simulate the LoS propagation for WPT.

Based on the above conditions, the results are drawn in Fig. 7. In general, the received power with RIS is larger than the received power without RIS for all algorithms, which indicates that RIS can improve the efficiency of received power even with the channel noise. When the SNR reaches 0 dB, which represents a signal-to-noise ratio of 1:1, the received power of AP-RA is 99.77% of MC-RA. It can be observed that the AP-RA is robust to the channel noise. The AP-RA with imperfect channel information has higher received power than the GA algorithm. And MC-RA outperforms other algorithms because it only depends on the actual feedback instead of channel information. Such feedbacks are more reliable than imperfect channel information. However, when the SNR reaches 10 dB, the received power of AP-RA begins approaching MC-RA, since the noise is too low to have impact on AP-RA.

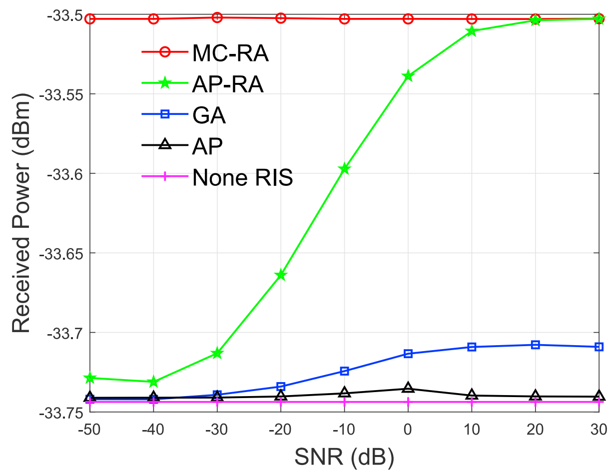

Fig. 7. Received power with different magnitude of the signal-to-noise ratio.

8.3. NLOS

One advantage of using RIS is to overcome the NLOS propagation. Here we compare the received power increase rate of four different passive beamforming algorithms. The received power increase rate is the ratio of received power of a typical beamforming algorithm between using RIS and without RIS. In addition, we also compare the received power increased rate between using RIS and without RIS in the LOS cases. We still implement our proposed AP-RA and MC-RA together with AP and GA. We set that the number of nodes is 20; the number of samples of the algorithm $M_S = 50$; the iteration number of all the algorithms is 200. We consider that there are obstacles between E-AP and the nodes. But there are no obstacles between E-AP and RIS, and no obstacles between RIS and the nodes as well. Thus, channel $\boldsymbol{c}$ is NLOS with a channel fading factor $\beta_{\text{NLOS}} = 1.2$, while $\boldsymbol{h}$ is LOS with a channel fading factor $\beta_{\text{LOS}} = 1$.

The received power increase rates of the four algorithms are presented in Fig. 8. With the same number of RIS, the received power increase rates of the EM based WPT system in the NLOS case are larger than in the LOS case. Note that, the results do not indicate that the NLOS cases attain more power than the LOS cases, but indicate a significant improvement in the NLOS cases. The power increase rate of MC-RA and AP-RA is much larger than the GA and AP algorithms. In the LOS case, the power increase rate of AP-RA is 22% and GA is 5.4%. In the NLOS case, the power increase rate of AP-RA is 246% but GA is 81%, which illustrates that the MC based random algorithm better compensates for the shortcomings brought by the NLOS propagation for WPT.

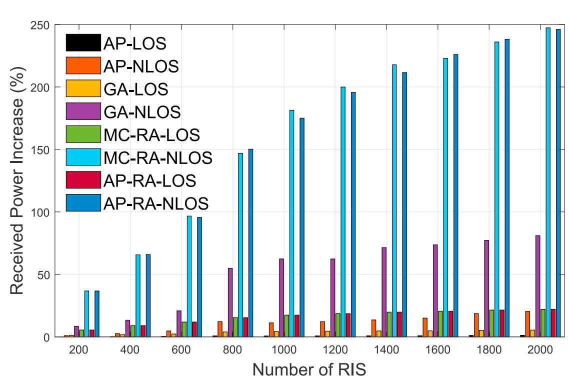

Fig. 8. The received power increase rate with different number of RIS reflective elements.

9. Conclusion

In this paper, we propose Monte-Carlo based random passive energy beamforming algorithms for RIS assisted WPT system, which can achieve the maximum received power. We first analyze that the phase shift of the RIS reflective element affects the received energy of the WPT system as a nonconvex integer programming problem. We obtain the approximation of the RIS reflective elements phase shift vector by estimation. Then we propose AP-RA based on channel information, which uses approximation as an initial passive beamforming solution and attains the optimal solution by iteratively calculation. Furthermore, we use MC-RA to cope with WPT systems without obtaining channel information. MC-RA drives the optimal beamforming solution based on the feedback from nodes. Through simulation analysis, compare with exhausting algorithm, MC-RA and AP-RA have better convergence accuracy, smaller complexity, and faster convergence rate. The received power attained by AP-RA is 15% larger than GA, and 22% larger than that in the none RIS case. If the channel information is available, AP-RA has a faster convergent rate than MC-RA. If the channel information contains many errors, MC-RA outperforms AP-RA since MC-RA does not depend on channel information but on actual received power feedback instead. In the NLOS case, the received power of AP-RA is 246% larger than that in the none RIS case and 91% larger than that of GA. Thus, in both LOS and NLOS cases, the AP-RA and MC-RA are feasible solutions for passive beamforming of RIS assisted wireless power transfer system.

Declaration of competing interest

The authors declare that they have no known competing financial interests or personal relationships that could have appeared to influence the work reported in this paper.

References

[1] D. Altinel, G. Karabulut Kurt, Modeling of multiple energy sources for hybrid energy harvesting iot systems, IEEE Internet Things J. 6 (6) (2019) 10846–10854.
[2] O. Cetinkaya, D. Balsamo, G.V. Merrett, Internet of mimo things: uav-assisted wireless-powered networks for future smart cities, IEEE Internet of Things Magazine 3 (1) (2020) 8–13.
[3] G. Ma, J. Xu, Y.-F. Liu, M.R.V. Moghadam, Time-division energy beamforming for multiuser wireless power transfer with non-linear energy harvesting, IEEE.Wireless.Commun.Lett. 10 (1) (2021) 53–57.
[4] B. Clerckx, R. Zhang, R. Schober, D.W.K. Ng, D.I. Kim, H.V. Poor, Fundamentals of wireless information and power transfer: from rf energy harvester models to signal and system designs, IEEE J. Sel. Area. Commun. 37 (1) (2019) 4–33.
[5] A.A. Eteng, H.H. Goh, S.K.A. Rahim, A. Alomainy, A review of metasurfaces for microwave energy transmission and harvesting in wireless powered networks, IEEE Access 9 (2021) 27518–27539.
[6] S. Luo, P. Yang, Y. Che, K. Yang, K. Wu, K.C. Teh, S. Li, Spatial modulation for ris-assisted uplink communication: joint power allocation and passive beamforming design, IEEE Trans. Commun. 69 (10) (2021) 7017–7031.
[7] A. Bhowal, S. Aissa, R. Singh Kshetrimayum, Ris-assisted spatial modulation and space shift keying for ambient backscattering communications, in: ICC 2021 - IEEE International Conference on Communications, 2021, pp. 1–6.
[8] J. Chen, Y. Xu, Q. Wu, Y. Zhang, X. Chen, N. Qi, Interference-aware online distributed channel selection for multicluster fanet: a potential game approach, IEEE Trans. Veh. Technol. 68 (4) (2019) 3792–3804.
[9] W. Tang, M.Z. Chen, X. Chen, J.Y. Dai, Y. Han, M. Di Renzo, Y. Zeng, S. Jin, Q. Cheng, T.J. Cui, Wireless communications with reconfigurable intelligent surface: path loss modeling and experimental measurement, IEEE Trans. Wireless Commun. 20 (1) (2021) 421–439.
[10] B. Clerckx, J. Kim, K.W. Choi, D.I. Kim, Foundations of wireless information and power transfer: theory, prototypes, and experiments, Proc. IEEE 110 (1) (2022) 8–30.
[11] A.A.G. Amer, S.Z. Sapuan, N. Nasimuddin, A. Alphones, N.B. Zinal, A comprehensive review of metasurface structures suitable for rf energy harvesting, IEEE Access 8 (2020) 76433–76452.
[12] Y. Xu, Z. Gao, Z. Wang, C. Huang, Z. Yang, C. Yuen, Ris-enhanced wpcns: joint radio resource allocation and passive beamforming optimization, IEEE Trans. Veh. Technol. 70 (8) (2021) 7980–7991.
[13] M. Jung, W. Saad, M. Debbah, C.S. Hong, On the optimality of reconfigurable intelligent surfaces (riss): passive beamforming, modulation, and resource allocation, IEEE Trans. Wireless Commun. 20 (7) (2021) 4347–4363.
[14] W. Yan, X. Yuan, Z.-Q. He, X. Kuai, Passive beamforming and information transfer design for reconfigurable intelligent surfaces aided multiuser mimo systems, IEEE J. Sel. Area. Commun. 38 (8) (2020) 1793–1808.

[15] H. Song, M. Zhang, J. Gao, C. Zhong, Unsupervised learning-based joint active and passive beamforming design for reconfigurable intelligent surfaces aided wireless networks, IEEE Commun. Lett. 25 (3) (2021) 892–896.
[16] X. Ma, S. Guo, H. Zhang, Y. Fang, D. Yuan, Joint beamforming and reflecting design in reconfigurable intelligent surface-aided multi-user communication systems, IEEE Trans. Wireless Commun. 20 (5) (2021) 3269–3283.
[17] K. Feng, Q. Wang, X. Li, C.-K. Wen, Deep reinforcement learning based intelligent reflecting surface optimization for miso communication systems, IEEE.Wireless.Commun.Lett. 9 (5) (2020) 745–749.
[18] L. Mohjazi, S. Muhaidat, Q.H. Abbasi, M.A. Imran, O.A. Dobre, M. Di Renzo, Battery recharging time models for reconfigurable intelligent surfaces-assisted wireless power transfer systems, IEEE.Trans.Green.Commun. Netw. 5 (2021) 145–161.
[19] N.M. Tran, M. Miftahul Amri, J.H. Park, D. In Kim, K.W. Choi, Beam scanning methods for multi-antenna wireless power transfer with reconfigurable intelligent surface, in: 2021 IEEE 22nd International Workshop on Signal Processing Advances in Wireless Communications, SPAWC, 2021, pp. 626–630.
[20] K. Li, Y. Naderi, U. Muncuk, K.R. Chowdhury, isurface: self-powered reconfigurable intelligent surfaces with wireless power transfer, IEEE Commun. Mag. 59 (11) (2021) 109–115.
[21] N.M. Tran, M.M. Amri, J.H. Park, D.I. Kim, K.W. Choi, Multi-device charging ris-aided wireless power transfer systems, in: 2021 International Conference on Information and Communication Technology Convergence, ICTC), 2021, pp. 839–844.
[22] H. Yang, X. Yuan, J. Fang, Y.-C. Liang, Reconfigurable intelligent surface aided constant-envelope wireless power transfer, IEEE Trans. Signal Process. 69 (2021) 1347–1361.
[23] S. Gong, Z. Yang, C. Xing, J. An, L. Hanzo, Beamforming optimization for intelligent reflecting surface-aided swipt iot networks relying on discrete phase shifts, IEEE Internet Things J. 8 (10) (2021) 8585–8602.
[24] S. Lin, B. Zheng, G.C. Alexandropoulos, M. Wen, M. di Renzo, F. Chen, Joint passive beamforming and information transfer for ris-empowered wireless communications, in: GLOBECOM 2020 - 2020 IEEE Global Communications Conference, 2020, pp. 1–6.
[25] A. Li, Y. Liu, M. Li, Q. Wu, J. Zhao, Joint scheduling design in wireless powered mec iot networks aided by reconfigurable intelligent surface, in: 2021 IEEE/CIC International Conference on Communications in China, ICCC Workshops), 2021, pp. 159–164.
[26] Z. Yang, Y. Zhang, Optimal swipt in ris-aided mimo networks, IEEE Access 9 (2021) 112552–112560.
[27] Z. Gao, Y. Xu, Q. Wang, Q. Wu, D. Li, Outage-constrained energy efficiency maximization for ris-assisted wpcns, IEEE Commun. Lett. 25 (10) (2021) 3370–3374.
[28] S. Lin, F. Chen, M. Wen, Y. Feng, M. Di Renzo, Reconfigurable intelligent surface-aided quadrature reflection modulation for simultaneous passive beamforming and information transfer, IEEE Trans. Wireless Commun. 6 (1) (2021) 75–89.
[29] S. Lin, M. Wen, M. Di Renzo, F. Chen, Reconfigurable intelligent surface-based quadrature reflection modulation, in: ICC 2021 - IEEE International Conference on Communications, 2021, pp. 1–6.
[30] S. Lin, B. Zheng, G.C. Alexandropoulos, M. Wen, M.D. Renzo, F. Chen, Reconfigurable intelligent surfaces with reflection pattern modulation: beamforming design and performance analysis, IEEE Trans. Wireless Commun. 20 (2) (2021) 741–754.
[31] Y. Pan, K. Wang, C. Pan, H. Zhu, J. Wang, Self-sustainable reconfigurable intelligent surface aided simultaneous terahertz information and power transfer (stipt), IEEE Trans. Wireless Commun. 2 (2022) 145–151.
[32] H. Ren, Z. Zhang, Z. Peng, L. Li, C. Pan, Energy minimization in ris-assisted uav-enabled wireless power transfer systems, IEEE Internet Things J. 5 (2022) 12–18.
[33] Y. Cheng, W. Peng, C. Huang, Y. Xu, C. Yuen, Ris-aided wireless power transfer for unmanned aerial vehicles, in: 2021 13th International Conference on Wireless Communications and Signal Processing, WCSP), 2021, pp. 1–5.
[34] Y. Zhao, X. Li, H. Wu, C.-Z. Xu, Energy beamforming for cooperative localization in wireless-powered communication network, IEEE Internet Things J. 8 (17) (2021) 13750–13762.
[35] J.S. Liu, W.A. Kong, Covariance structure and convergence rate of the gibbs sampler with various scans, J. Roy. Stat. Soc. 57 (1) (1995) 157–169.
[36] U. Wolff, Monte Carlo errors with less errors, Comput. Phys. Commun. 156 (2) (2004) 143–153.
[37] N.J. Gordon, D.J. Salmond, A. Smith, Novel approach to nonlinear/non-Gaussian bayesian state estimation, IEE Proc. - Part F .Radar Signal Process. 140 (2) (1993) 107–113.
[38] F.A. Potra, Onq-order andr-order of convergence, J. Optim. Theor. Appl. 63 (3) (1989) 415C431.